Numerical Simulation of Thermal Atmospheric Conditions in an Idealized Street Canyon: Comparison Between RANS and LES

A. W. Muhammad Yazid[*,1,a], *S. M. Salim*[2,b] *and S. Mansor*[3,c]

[1]Department of Thermo-Fluids, Faculty of Mechanical Engineering, Universiti Teknologi Malaysia, 81310 Skudai, Johor Bahru, Malaysia
[2]School of Engineering and Physical Sciences, Heriot-Watt University Malaysia, 62100 Putrajaya, Malaysia
[3]Department of Aeronautics, Automotive & Ocean Engineering, Faculty of Mechanical Engineering, Universiti Teknologi Malaysia, 81310 Skudai, Johor Bahru, Malaysia

[a,*]*afiqwitri@gmail.com,* [b]*m.salim@hw.ac.uk,* [c]*shuhaimi@fkm.utm.my*

Abstract – *This paper reports on the numerical comparison for the prediction of wind flow structure under thermal atmospheric conditions between a steady state Reynolds-averaged Navier-Stokes (RANS) model (the standard k-ε) and a large eddy simulation (LES) technique with dynamic Smargorinsky-Lilly subgrid-scale (SGS) model against the previous experimental wind tunnel data. Two cases of thermal conditions are investigated, one for a different Fr number with leeward heated wall (isothermal, Fr=17.29, Fr=7.59) and another for a different location of heated wall (windward). The results of the numerical simulation indicate that the LES performs better than RANS by accurately predict the wind flow structure at different thermal intensites and different locations of heated wall.* *Copyright © 2014 Penerbit Akademia Baru - All rights reserved.*

Keywords: Idelized street canyon, Thermal atmospheric conditions, RANS, LES

1.0 INTRODUCTION

Thermal stability can be categorized as stable, neutral (isothermal), and unstable and it requires parameters such as ground temperature and wind speed to distinguish different thermal stability regimes [1]. Differential wall heating due to solar angle also reflects the thermal condition in street canyon. In general, the stable condition yields low wind speed in street canyon while condition with ground heating causes high wind speed. With regards to the differential wall heating of unstable atmospheric condition, if the windward wall is involved in multiple wall heating, the vortex intensity is slightly weakened while leeward and/or ground heated wall will intensify the vortex strength [2]. The location of heated wall also varies the resultant wind flow structure in the street canyon [3].

Previous experimental study is limited to very few numbers of thermal atmospheric conditions, for example exclusive effect of windward wall heated only [4] or ground heated only [5]. In addition, previous validation studies [6, 2, 7] are limited to very few number of turbulence models and for very few thermal conditions. There is high uncertainty whether the chosen turbulent model could predict the airflow under various thermal atmospheric conditions correctly. Recent experimental work by Allegrini et al [8] on thermal flow in street canyon has provided more data on the airflow structure in street canyon under different thermal conditions. Therefore, the dataset of wind tunnel study by Allegrini et al [8] is used as a benchmark to find

a universal turbulent model that can simulate airflow in urban street canyon under various thermal atmospheric conditions.

Numerical validation between one two-equation Reynolds-Averaged Navier-Stokes (RANS) turbulent model of standard k-ε and one large eddy simulation (LES) technique of dynamic Smargorinsky-Lilly subgrid scale (SGS) model against wind tunnel (WT) experiment is investigated in this paper. The purpose was to determine whether the chosen turbulence models are able to simulate wind flow structure under different atmospheric conditions. This could help other researchers in choosing an appropriate turbulent model to simulate wind flow in street canyon under thermal atmospheric conditions.

2.0 METHODOLOGY

The numerical models were validated against the wind tunnel experiment of Allegrini et al [8] where the incoming wind flow is characterized by the Reynolds number, defined as in (1) while the thermal flow is characterized by the Froude (Fr) number, defined as in (2) where g is the acceleration due to gravity (m/s^{-2}), H is the depth of cavity (m), T_w is the heated wall temperature (K), T_{ref} and U_{FS} are the ambient temperature (K) and free stream velocity (m/s) respectively.

$$\text{Re} = \frac{\rho U_{FS} H}{\mu} \tag{1}$$

$$\text{Fr} = \frac{U_{FS}^2}{gH \dfrac{T_w - T_{ref}}{T_{ref}}} \tag{2}$$

The flow is dominantly induced by buoyant force if Fr is low and is dominantly induced by convective flow if Fr is high. The flow direction was normal to the axis of the cavity and maintained at ambient temperature, $T_{ref} = 23˚C$ with free stream velocity, $U_{FS} = 2.32$ m/s for Re = 30700. Inlet velocity and turbulent kinetic energy profiles were estimated from WT inlet profiles using exponential law where the exponent for velocity is 0.11 while the exponent for turbulent kinetic energy is -0.317 (Figure 1). However, the estimated velocity profile is close to WT for height up to y/H=0.5 only and since the focus of the study is located below the shear layer, the estimated velocity profile is valid to be used in the present study. A relationship between turbulent kinetic energy and turbulence length scale were used to estimate the turbulent dissipation profile written as:

$$\varepsilon = C_\mu^{3/4} \frac{k^{3/2}}{\ell} \tag{3}$$

where C_μ is the empirical constant specified in the turbulence model (approximatly 0.09) and ℓ is the turbulence length scale, which approximated as $0.4\delta_{99}$ for wall-bounded flows where $\delta_{99} = 0.855$m as the height of the wind tunnel [9]. The flow conditions being studied were at Reynolds number, Re = 30700 with thermal conditions of isothermal flow, leeward heated wall at two Froude number (Fr = 17.29 and 7.59) and windward heated wall (Fr = 7.59).

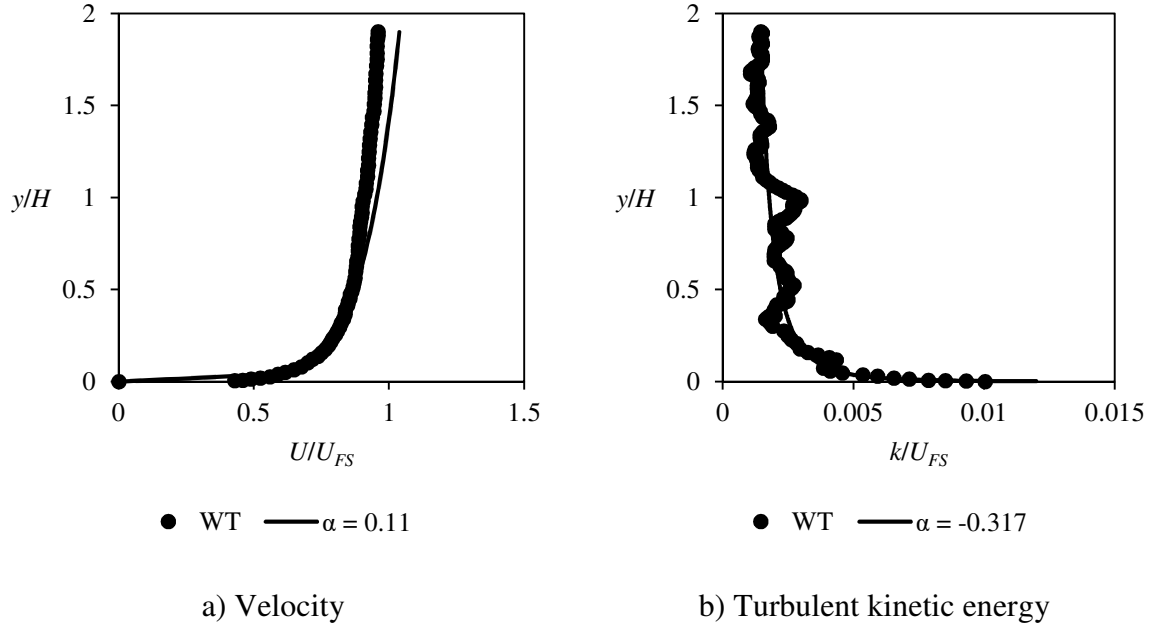a) Velocity   b) Turbulent kinetic energy

Figure 1: The variation of mean wind velocities with height from WT and from estimation using exponential law

A finite volume method of a commercial computational fluid dynamics software package, ANSYS FLUENT v14 was used by assuming incompressible with 3D spatial domain. The first study was conducted using standard k-ε (SKE) of two-equation steady-state RANS equations to solve the turbulence flow. Enhanced wall treatment was adopted due to its ability to accurately simulate buoyancy flow. Second order upwind for all the advection term, PRESTO for pressure interpolation and SIMPLE algorithm for the pressure-velocity coupling were used as discretization scheme for SKE. The convergence was monitored at 1.0×10^{-6} for isothermal case and 1.0×10^{-4} for thermal case. The mean and fluctuating components of velocity, pressure and temperature in the original continuity, Navier-Stokes and energy equations respectively, are separated by Reynolds averaging, and by taking a time average, yields the following govering quations as in (4), (5) and (6) assuming a steady-state condition. Additional governing equations are required as in (7) and (8) to mathermatically close the problem [10].

$$\frac{\partial \overline{u}_i}{\partial x_i} = 0 \tag{4}$$

$$\overline{u}_j \frac{\partial \overline{u}_i}{\partial x_j} = -\frac{1}{\rho}\frac{\partial \overline{p}}{\partial x_i} + \frac{\partial}{\partial x_j}\left[\nu \left(\frac{\partial \overline{u}_i}{\partial x_j} + \frac{\overline{u}_j}{\partial x_i} \right) - \overline{u_i' u_j'} \right] + g_j \left(\frac{\rho_w - \rho_{ref}}{\rho_{ref}} \right) \tag{5}$$

$$\overline{u}_i \frac{\partial \overline{T}}{\partial x_i} + \frac{\partial}{\partial x_i}\left(\overline{u_i' T'} \right) = 0 \tag{6}$$

$$\overline{u}_i \frac{\partial k}{\partial x_i} = \frac{1}{\rho}\frac{\partial}{\partial x_j}\left[\left(\mu + \frac{\mu_t}{\sigma_k} \right)\frac{\partial k}{\partial x_j} \right] + \frac{G_k}{\rho} + \frac{G_b}{\rho} - \varepsilon \tag{7}$$

$$\bar{u}_i \frac{\partial \varepsilon}{\partial x_i} = \frac{1}{\rho} \frac{\partial}{\partial x_j} \left[\left(\mu + \frac{\mu_t}{\sigma_\varepsilon} \right) \frac{\partial \varepsilon}{\partial x_j} \right] + \frac{1}{\rho} C_{1\varepsilon} \frac{\varepsilon}{k} \left(G_k + C_{3\varepsilon} G_b \right) - C_{2\varepsilon} \frac{\varepsilon^2}{k} \qquad (8)$$

where u_i is the velocity, x_i the spatial coordinates, p the pressure, v the kinetmatic viscosity, g the gravitational acceleration, ρ_0 is the ambient air density, and ρ_w is the air denisty near the heated wall. The model coefficients and model constants for SKE adopted in the present study are given in Table 1.

Table 1: The model coefficients and model constants for SKE

Coefficients	$\mu_t = \rho C_\mu \dfrac{k^2}{\varepsilon}$; $G_k = \mu_t S^2$; $G_b = \beta g_i \dfrac{\mu_t}{\mathrm{Pr}_t} \dfrac{\partial \bar{T}}{\partial x_i}$; $S = \sqrt{2 S_{ij} S_{ij}}$; $\beta = -\dfrac{1}{\rho} \left(\dfrac{\partial \rho}{\partial T} \right)_p$
Constants	$C_{1\varepsilon} = 1.44$; $C_{2\varepsilon} = 1.92$; $C_{3\varepsilon} = \tanh|v/u|$; $C_\mu = 1.44$; $C_{1\varepsilon} = 1.44$; $\sigma_k = 1$; $\sigma_\varepsilon = 1.3$

The second turbulent model used was dynamic Smagorinsky-Lilly SGS model of LES techniques. Bounded central difference for momentum, second order upwind for energy transport equations, PRESTO for pressure interpolation and SIMPLEC algorithm for pressure-velocity coupling were used as the discretization schemes for LES by considering the recommendations for numerical quality, stability and computing time [9, 11]. The convergence was monitored at 1.0×10^{-3}. Boussinesq approximation was used in both studies to simulate the buoyancy flow, and the wall was homogeneously heated up at constant temperature. In LES, the time-dependent flow variables are decomposed into the resolved-scale and the subgrid-scale through a spatial filtering operation. In ANSYS FLUENT, the box filter functions is employed, resulting in the filtered continuity, momentum and energy equtions as follows:

$$\frac{\partial \bar{u}_i}{\partial x_i} = 0 \qquad (9)$$

$$\frac{\partial \bar{u}_i}{\partial t} + \bar{u}_j \frac{\partial \bar{u}_i}{\partial x_j} = -\frac{1}{\rho} \frac{\partial \bar{p}}{\partial x_i} - \frac{\partial \tau_{ij}}{\partial x_j} + v \frac{\partial^2 \bar{u}_i}{\partial x_j \partial x_j} + \beta g_j \left(T_w - T_{ref} \right) \delta_{ij} \qquad (10)$$

$$\frac{\partial \bar{T}}{\partial t} + \bar{u}_i \frac{\partial \bar{T}}{\partial x_j} = \frac{\partial}{\partial x_j} \left(\frac{v}{\mathrm{Pr}} \frac{\partial \bar{T}}{\partial x_j} \right) - \frac{\partial h_j}{\partial x_j} \qquad (11)$$

where $\tau_{ij} = \overline{u_i u_j} - \bar{u}_i \bar{u}_j$ and $h_j = \overline{u_j T} - \bar{u}_j \bar{T}$ is the subgrid scale (SGS) turbulent stress and heat fluxes respectively, appeared as a results of the filtering operation which are unknown terms and require further modeling in order to mathematically close the problem. Unlike in RANS, the overbar in LES indicates spatial filtering. The SGS stress model employed by ANSYS FLUENT is based on the Boussinesq hypothesis in which the SGS stress is express in the form of:

$$\tau_{ij} = -2 v_{SGS} \bar{S}_{ij} + \frac{1}{3} \tau_{kk} \delta_{ij} \qquad (12)$$

where v_{SGS} is the SGS eddy-viscosity viscosity, $\bar{S}_{ij}$ is the rate of strain tensor for the resolved scale and other coefficients and constants are defined as in Table 2 while τ_{kk} term is neglected assuming incompressible flows [12]. The eddy viscosity is modeled according to the Smagorinsky-Lilly model [13] and the Smagorinsky model constant, C_s is dynamically

computed following the procedure of Germano et al., 1991 [14] and Lilly [15] based on the information provided by the resolved scales of motion, thus obviates the needs to specify the model constant C_s in advance.

Table 2: The model coefficients and model constants for LES

Coefficients	$v_{SGS} = \rho L_s^2 \left|\overline{S}\right|$; $\overline{S}_{ij} = \dfrac{1}{2}\left(\dfrac{\partial \overline{u}_i}{\partial x_j} + \dfrac{\partial \overline{u}_j}{\partial x_i}\right)$; $\left|\overline{S}\right| = \sqrt{2\overline{S}_{ij}\overline{S}_{ij}}$; $L_s = \min\left(kd, C_s V^{1/3}\right)$; $h_j = \dfrac{v_{SGS}}{\text{Pr}_{SGS}}\dfrac{\partial \overline{T}}{\partial x_j}$
Constants	C_s = Smagorinsky constant; k = von Karman constant (0.4); d is the distance to the closest wall; V is the volume of the computational cell; Pr_{SGS} = subgrid Prandtl number (0.85)

The numerical domain of street canyon model has the aspect ratio of 1 (height to width ratio) with dimensions of 0.2 (*H*) x 0.2 (*W*) x 1.8 (*L*) m. The thermal conditions led to the similar conditions of real scale at 1:100. The computational domain and boundary conditions used for the current study are shown in Figure 2. Since the length of the canyon model and the height of the WT are relatively long compared to the canyon model height and width, symmetry boundary condition was imposed at the top and spanwise of current computational domain limit, assuming that the domain is far enough to have an effect on the flow structure within the street canyon. The whole domain was discretized using hexahedral elements while the overlying cavity was stretched away from the cavity with 1.2 ratio, and the spatial resolutions are listed in Table 3.
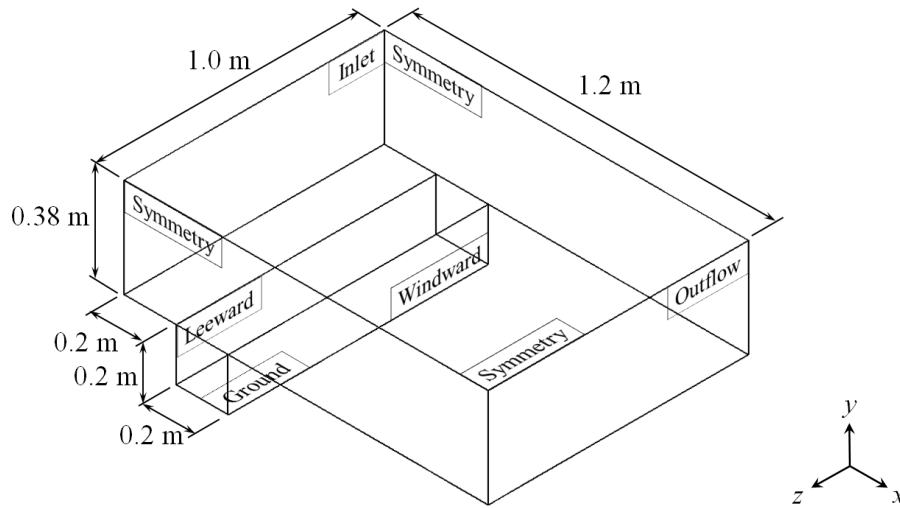

Figure 2: Schematic diagram of the computational domain and boundary conditions

The time resolution used in the current study was based on the requirement of Courant-Friedrichs-Levy (CFL) number of CFL = $U\Delta t/\Delta x < 1$ where U is about 0.7 m/s at roof level and Δx is the smallest element size. Hence, $\Delta t = 0.000143$ s was used which suffices for the CFL requirements. Firstly, a steady state simulation using SKE was obtained and the steady state statistics was used as the initial conditions for the LES simulation. The LES simulation

was continued for $100H/U$ of dimensionless simulation time where H is the depth of cavity and U is the speed at roof level in order to establish the turbulent wind fields throughout the domain, and all statistics were averaged at least for $50H/U$.

Table 3: Mesh resolution used in the current computational fluid dynamics study

Mesh	Number of cells in street canyon ($x \times y \times z$)	Total number of cells
Mesh 1	$30 \times 30 \times 150$	340k
Mesh 2	$40 \times 40 \times 150$	533k
Mesh 3	$70 \times 70 \times 150$	1M

3.0 RESULTS AND DISCUSSION

A series of model sensitivity tests were first conducted to determine an optimum spatial resolution and the required period of time as to achieve a statistically steady state for LES simulation while for SKE, the model sensitivity has been conducted in previous study [6]. For mesh independent study, data of streamwise velocity at 4 locations taken along the vertical middle of the street which are 0.04 m (1), 0.08 m (2), 0.12 m (3) and 0.16 m (4) from the ground were plotted against the total number of cells (Figure 3). Mesh 2 with cell size near wall of 0.025H was enough to resolve the overall flow fields as there are no abrupt wind flow variations with more grid cells (Mesh 3). An averaged value of $50H/U$ simulation time at 2 different time (after $100H/U$ and $150H/U$) at 4 locations taken along the vertical middle of the street which are 0.04 m (1), 0.08 m (2), 0.12 m (3) and 0.16 m (4) from the ground were compared to determine the statistically steady state. The root mean square of streamwise velocity is about 0.013 m/s which is relatively small compared to 0.1 m/s suggested by Beare et al [16].
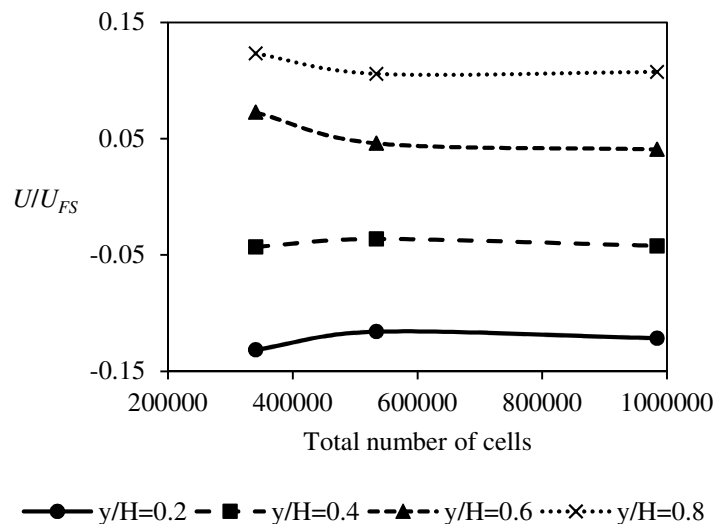

Figure 3: Streamwise velocity along the vertical middle of street canyon under different thermal flow conditions

The result of validation study for isothermal and leeward wall heated condition at two Fr number is shown in Figure 4. The streamwise velocity data was normalized by freestream velocity, $U_{FS} = 2.32$ m/s. In all cases, the LES results showed a good approximation with the

experiment while the SKE had failed in all cases. Further calculation of deviation between SKE and LES against WT (Table 4) shows increased of velocity for both SKE and LES but is more significant when the former turbulent model was used.
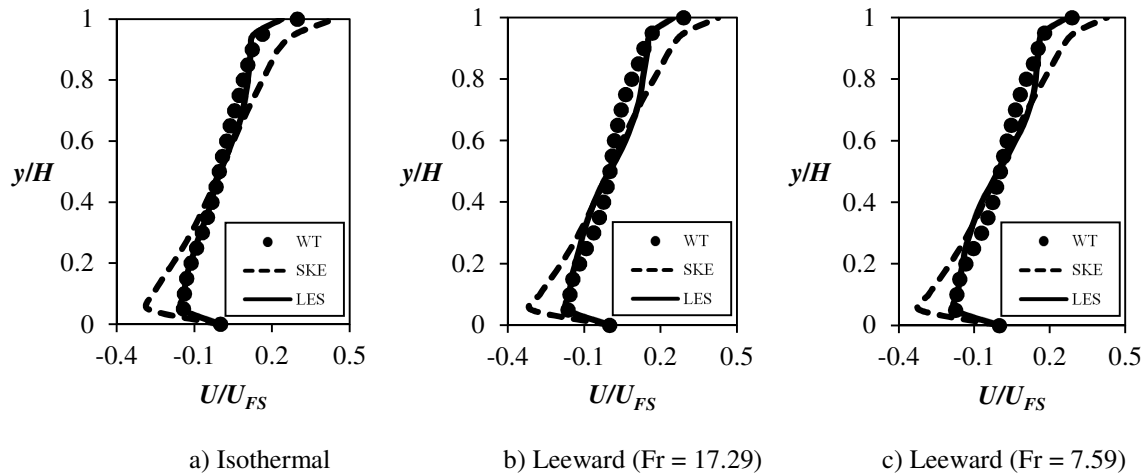

a) Isothermal   b) Leeward (Fr = 17.29)   c) Leeward (Fr = 7.59)

Figure 4: Normalized streamwise velocity along the vertical middle of street canyon under different thermal flow conditions

The wind flow fields under windward heated wall conditions showed more complex wind flow structure. At Fr=7.59 and Re=30700, 3 vortices were produced within the street canyon (Figure 5b). The primary vortex circulated in clockwise motion driven by the shear layer and located at the right top corner of the canyon. The secondary vortex was located at the right bottom corner of the canyon with anti-clockwise motion, driven by the primary vortex. A relatively small tertiary vortex was in an anti-cockwise motion driven by both the primary and secondary vortices.

Figure 5 shows the contour of velocity magnitude and vector plot for WT, SKE and LES. It is clear that the LES can well reproduce the flow field while the SKE results show significantly higher velocity magnitude. Further inspection on the vortex centroid for each vortex (Table 5) shows that SKE has failed to reproduce both the secondary and tertiary vortices as in WT. Not only LES is able to reproduce all the vortices but the location of vortex centroid is also close to WT results.

Table 4: Average error of streamwise velocity along the vertical middle of street canyon for validation study

Simulation Case	Isothermal		Leeward (Fr = 17.59)		Leeward (Fr = 7.59)	
Turbulence model	SKE	LES	SKE	LES	SKE	LES
Average error (%)	78.3	33.5	118.1	86.2	80.7	64.5

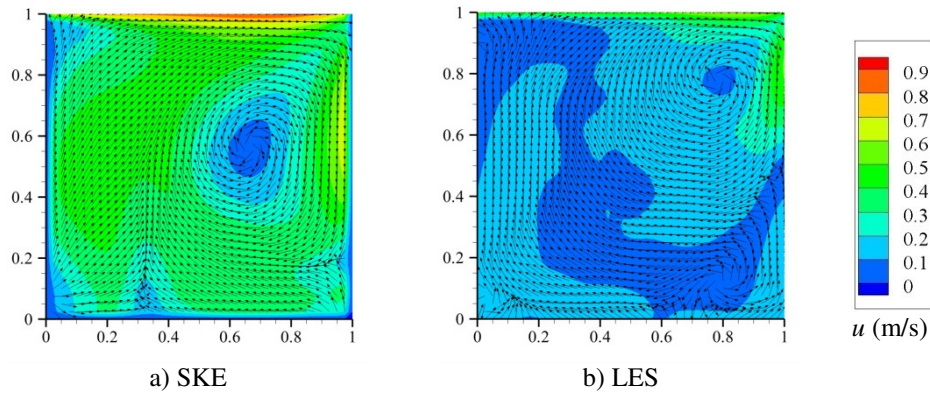a) SKE   b) LES

Figure 5: Contour and vector plot of velocity magnitude of windward wall heated at Fr = 7.59

Table 5: Vortex centroid of windward heated wall at Fr = 7.59

Type of vortex	Vortex centroid (x, y)		
	WT	SKE	LES
Primary vortex	0.736, 0.736	0.673, 0.564	0.751, 0.766
Secondary vortex	0.850, 0.189	-	0.771, 0.122
Tertiary vortex	0.076, 0.057	-	0.034, 0.063

4.0 CONCLUSION

Validation study between SKE and LES against WT on the airflow structure within street canyon of aspect ratio one was performed to determine the best turbulent model for the prediction of thermal flow in street canyon. Results obtained shows that LES can well calculate a complex simulation involving isothermal flow and thermal flow with different thermal intensity and different heat location by producing lower deviation and predicted a good wind flow structure against WT. Therefore, LES is highly recommended to be use a turbulent technique to perform thermal and turbulent flow in street canyon settings.

REFERENCES

[1]   A.W.M. Yazid, N.A.C. Sidik, S.M. Salim, K.M. Saqr, A review on the flow structure and pollutant dispersion in urban street canyons for urban planning strategies, Simulation: Transactions of the Society for Modeling and Simulation International 40 (8) (2014) 892–916.

[2]   X. Xie, C.-H. Liu, D.Y.C. Leung, Impact of building facades and ground heating on wind flow and pollutant transport in street canyons, Atmospheric Environment 41 (39) (2007) 9030–9049.

[3]   J.J. Kim, J.J. Baik, A numerical study of thermal effects on flow and pollutant dispersion in urban street canyons, Journal of Applied Meteorology 38 (9) (1999) 1249–1261.

[4]   A. Kovar-Panskus, L. Moulinneuf, E. Savory, A. Abdelqari, J.-F. Sini, J.-M. Rosant, A. Robins, N. Toy, A wind tunnel investigation of the influence of solar-induced wall heating on the flow regime within a simulated urban street canyon, Water, Air and Soil Pollution: Focus 2 (5-6) (2002) 555–571.

[5]   K. Uehara, S. Murakami, S. Oikawa, Wind tunnel experiments on how thermal stratification affects flow in and above urban street canyons, Atmospheric Environment 34 (10) (2000) 1553–1562.

[6]   A.W.M. Yazid, N.A.C. Sidik, S.M. Salim. Numerical simulation of wind flow structures and pollutant dispersion within street canyon under thermally unstable atmospheric conditions, Applied Mechanics and Materials, 554 (2014) 655–659.

[7]   X.-M. Cai. Effects of differential wall heating in street canyons on dispersion and ventilation characteristics of a passive scalar, Atmospheric Environment 51 (2012) 268-277.

[8]   J. Allegrini, V. Dorer, J. Carmeliet, Wind tunnel measurements of buoyant flows in street canyons, Building and Environment 59 (2013) 315–326.

[9]   Ansys Inc., ANSYS FLUENT User's Guide (2011).

[10] B.E. Launder, D.B. Spalding, The numerical computation of turbulent flows, Computer Methods in Applied Mechanics and Engineering, 3 (2) (1974) 269-289.

[11] J. Franke, A. Hellsten, H. Schlünzen, B. Carissimo, Best practice guideline for the CFD simulation of flows in the urban environment, COST 732: Quality Assurance and Improvement of Microscale Meteorological Models, 2007.

[12] Ansys Inc., ANSYS FLUENT Theory Guide (2011).

[13] J. Smagorinsky, General circulation experiments with the primitive equations, Experiment, Monthly Weather Review 91 (3) (1963) 99–164.

[14] M. Germano, U. Piomelli, P. Moin, W.H. Cabot, A dynamic subgrid-scale eddy viscosity model, Physics of Fluids A: Fluid Dynamics 3 (7) (1991) 1760–1765.

[15] D.K. Lilly, A proposed modification of the Germano subgrid-scale closure method, Physics of Fluids A: Fluid Dynamics 4 (3) (1992) 633–635.

[16] R.J. Beare, M.K. Macvean, A.A.M. Holtslag, J. Cuxart, I. Esau, J.-C. Golaz, M. A. Jimenez, M. Khairoutdinov, B. Kosovic, D. Lewellen, T.S. Lund, J. K. Lundquist, A. Mccabe, A.F. Moene, Y. Noh, S. Raasch, P. Sullivan, An intercomparison of large-eddy simulations of the stable boundary layer, Boundary-Layer Meteorology 118 (2) (2006) 247-272.